International Journal of Automotive Technology, Vol. 6, No. 6, pp. 599–605 (2005)

1229-9138/2005/024-07

DEVELOPMENT OF VEHICLE DYNAMICS MODEL FOR REAL-TIME ELECTRONIC CONTROL UNIT EVALUATION SYSTEM USING KINEMATIC AND COMPLIANCE TEST DATA

S. S. KIM[1)*], H. K. JUNG[2)], J. S. SHIM[3)] and C. W. KIM[3)]

[1)]Graduate School of Automotive Engineering, Kookmin University, Seoul 126-702, Korea
[2)]Hyundai Motor Company, 772-1 Jangduk-dong, Whasung-si, Gyeonggi 445-706, Korea
[3)]Seomoon Technologies, Inc., 7th FL., Seohyeon Leaders Building, 274-4 Seohyeon-dong, Bundang-gu, Seongnam-si, Gyeonggi 463-824, Korea

(Received 7 October 2004; Revised 22 July 2005)

ABSTRACT–A functional suspension model is proposed as a kinematic describing function of the suspension, that represents the relative wheel displacement in polynomial form in terms of the vertical displacement of the wheel center and steering rack displacement. The relative velocity and acceleration of the wheel is represented in terms of first and second derivatives of the kinematic describing function. The system equations of motion for the full vehicle dynamic model are systematically derived by using velocity transformation method of multi-body dynamics. The comparison of test and simulation results demonstrates the validity of the proposed functional suspension modeling method. The model is computationally very efficient to achieve real-time simulation on TMS 320C6711 150 MHz DSP board of HILS (hardware-in-the-loop simulation) system for ECU (electronic control unit) evaluation of semi-active suspension.

KEY WORDS : Vehicle dynamics model, Suspension model, Real-time simulation, ECU evaluation system, Kinematic and compliance test

1. INTRODUCTION

The application of real-time ECU (electronic control unit) evaluation system for development of vehicle electronic control systems has many advantages. It is an effective way to reduce expensive filed tests, evaluate interactions between chassis subsystems, and shorten the developing period of the vehicle. This system requires real-time vehicle dynamics model that describes vehicle's behavior accurately under various driving conditions.

The modeling approach for vehicle dynamic analysis can be divided into two types ; the multi-body model and parametric model. The multi-body model can accurately represent the kinematic and compliance characteristics of the suspension. However, this type of the model can be constructed when detailed component data such as suspension hard-points, spring and damping characteristic, the stiffness of rubber bushings, and the mass and inertia data of suspension links, are available. Another disadvantage of the multi-body model is computational inefficiency. The multi-body vehicle dynamics model with detailed suspension model is not suitable for real-time HILS (hardware-in-the-loop simulation) system.

The parametric model of the vehicle is a relatively simple model. Computer software such as VDANL (Allen *et al.*, 1987) and CarSim (Sayers and Han, 1996) uses a parametric suspension model. This model defines the kinematic characteristics of the suspension as gradients or curve data of wheel rotation angle (toe, camber, side view spin angle) in terms of the vertical motion of the wheel center. This type of modeling approach is suitable for real-time simulation, but the suspension model is not able to accurately model roll center migration, anti-dive, and jacking force due to the three dimensional kinematic characteristics of the suspension.

The objective of this paper is to develop a reduced order multi-body vehicle dynamic model for real-time simulation, that includes a more accurate representation of kinematic and compliance characteristics of suspension.

This paper defines the functional suspension model that represents the amount of change of the relative wheel displacement with respect to the car body as a function of the vertical displacement of the wheel center and steering rack displacement (Kim and Jung, 2000; 2004). The

*Corresponding author. e-mail: sskim@kookmin.ac.kr

kinematic describing function of the suspension is used to derive the equations for the motion of the vehicle. The equations of motion for the full vehicle model are systematically derived using the velocity transformation method of multi-body dynamics (Kim and Vanderploeg, 1986). The validity of the proposed method is demonstrated by comparing the simulation results of the functional suspension model with those of the multi-body vehicle model and field test results (MSC.ADAMS, 2003). A HILS system for ECU evaluation of semi-active suspension is constructed to demonstrate the effectiveness of the vehicle dynamics model.

2. VEHICLE KINEMATICS

The spatial motion of the vehicle is described by the position and orientation of the reference frames of the car body and wheels with respect to the inertial reference frame, as shown in Figure 1.

The motion of the wheel is described in the car body reference frame as the relative motion respect to the car body. The relative location and orientation angle of the wheel is represented as $Z'_{w/b} = \left[r'^{T}_{w/b},\ \theta'^{T}_{w/b}\right]^{T}$.

2.1. Relative Motion of the Wheel

The position of the wheel reference frame is described by the position vector

$$r'_w = A_{wb} r'_b + A_{wb} r'_{w/b} \tag{1}$$

where

$$A_{wb} = A_w{}^T A_b = A_{\alpha\beta\gamma}(\theta_{w/b})$$

where A_w and A_b represent transformation matrix, $A_{\alpha\beta\gamma}(\theta_{w/b})$ is rotation matrix of the wheel with respect to car body, and $\theta_{w/b}$ is the relative Euler angles such as toe, camber, and side view spin.

The time derivative of the relative position vector of the wheel is written as

$$\dot{y}'_{w/b} = \begin{bmatrix} \dot{r}'_{w/b} \\ \dot{\theta}'_{w/b} \end{bmatrix} = \begin{bmatrix} I & 0 \\ 0 & K_{w/b} \end{bmatrix} \begin{bmatrix} \dot{r}'_{w/b} \\ \dot{\omega}'_{w/b} \end{bmatrix} \tag{2}$$

where $K_{w/b}$ matrix is the function of the relative Euler angles of the wheel. Since these angles less than 2 degrees in the normal driving, $K_{w/b}$ can be assumed as identity matrix. Thus, we use this assumption in the following derivation.

$$\dot{Z}'_{w/b} = \dot{y}'_{w/b} \tag{3}$$

2.2. Relative Velocity of the Wheel

The local velocity vector of the wheel is written as

$$\begin{aligned} \dot{r}'_w &= A_{wb}\dot{r}'_b + A_{wb}\dot{r}'_{w/b} - A_{wb}\tilde{r}'_{w/b}\omega'_b \\ \omega'_w &= A_{wb}\omega'_b + A_{wb}\omega'_{w/b} \end{aligned} \tag{4}$$

where $\tilde{a}b$ represents cross product of two vectors.

In the symbolic form, the velocity vector is written as

$$\dot{y}'_w = D\dot{y}'_b + E\dot{y}'_{w/b} \tag{5}$$

where

$$\dot{y}'_b = \left[\dot{r}'^{T}_b,\ \dot{\theta}'^{T}_b\right]^{T}$$

$$\dot{y}'_w = \left[\dot{r}'^{T}_w,\ \dot{\theta}'^{T}_w\right]^{T}$$

$$\dot{y}'_{w/b} = \left[\dot{r}'_{w/b}{}^{T},\ \dot{\theta}'_{w/b}{}^{T}\right]^{T}$$

$$D = \begin{bmatrix} A_{wb} & -A_{wb}\tilde{r}'_{w/b} \\ 0 & A_{wb} \end{bmatrix}$$

$$E = \begin{bmatrix} A_{wb} & 0 \\ 0 & A_{wb} \end{bmatrix}$$

2.3. Relative Acceleration of the Wheel

The time derivative of equation (5) gives the local acceleration vector of the wheel

$$\ddot{y}'_w = D\ddot{y}'_b + E\ddot{y}'_{w/b} + h_1 \tag{6}$$

where

$$h_1 = \begin{bmatrix} 2A_{wb}\tilde{\omega}'_b\dot{r}'_{w/b} + A_{wb}\tilde{\omega}'_b\tilde{\omega}'_b r'_{w/b} \\ 0 \end{bmatrix}$$

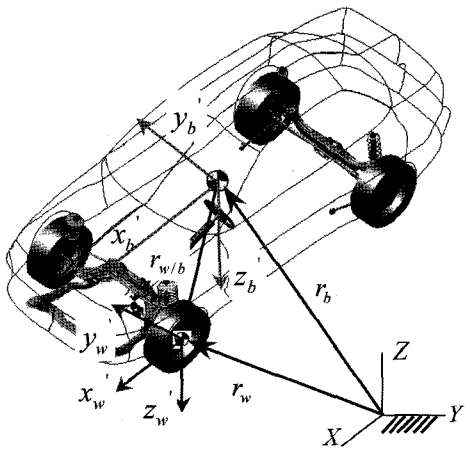

Figure 1. Reference frames of a vehicle.

3. FUNCTIONAL SUSPENSION MODEL

The relative position of the wheel center and the orientation of the wheel reference frame depends on the kinematic and compliance characteristics of the suspension. The kinematic and compliant deflection of the vehicle suspension can be measured on an kinematic and compliance (K&C) tester (Coovert *et al.*, 1992) or by using ADAMS/Car suspension test rig, as shown in Figure 2.

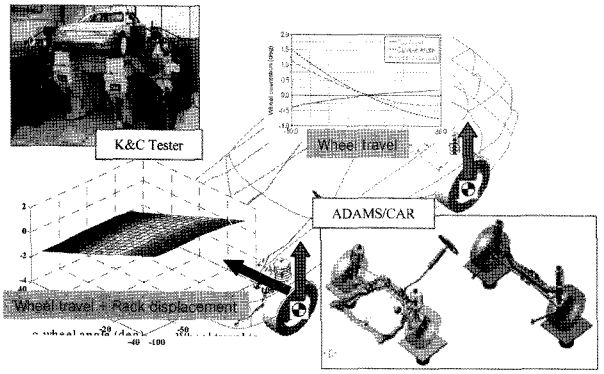

Figure 2. Methods to obtain suspension characteristics.

The kinematic tests measure wheel position changes that occur due to vehicle position changes such as ride height and roll. The steering tests measure wheel position changes due to steering wheel input at the given vehicle height. Compliance tests measure wheel position changes due to longitudinal and lateral force and aligning moment inputs (Choi *et al.*, 2005).

3.1. Parameterization of Suspension Kinematics

In order to parameterize the relative displacement of the wheel, independent coordinates for the suspension kinematics are wheel vertical displacement δ_w and steering rack displacement s_r in the case of steerable suspension. Non-steerable suspension needs the wheel vertical displacement as independent coordinates.

$$Z'_{w/b} = Z'_{w/b}(\delta_w,\ s_r) \quad \text{for steerable suspension} \tag{7}$$

$$Z'_{w/b} = Z'_{w/b}(\delta_w) \quad \text{for non-steerable suspension} \tag{8}$$

For the steerable suspension each of the relative wheel displacement is represented as a surface, shown in Figure 3. For example the toe angle can be described by a 3rd order polynomial in terms of δ_w and s_r.

$$\begin{aligned}\gamma'_{w/b} = &\left(a_3\delta_w{}^3 + a_2\delta_w{}^2 + a_1\delta_w\right) + \left(b_3 s_r{}^3 + b_2 s_r{}^2 + b_1 s_r\right) \\ &+ \left(c_1\delta_w{}^2 s_r + c_1\delta_w s_r{}^2 + c_3\delta_w s_r\right) + d\end{aligned} \tag{9}$$

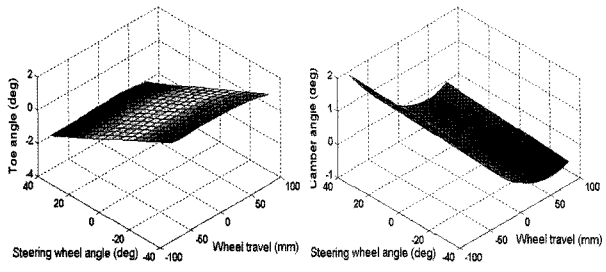

Figure 3. Suspension characteristics due to wheel travel and steering wheel angle input.

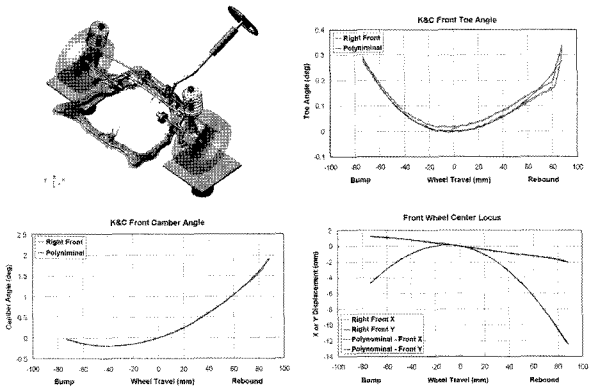

Figure 4. Front McPherson-Strut suspension K&C test results and polynomial fitting.

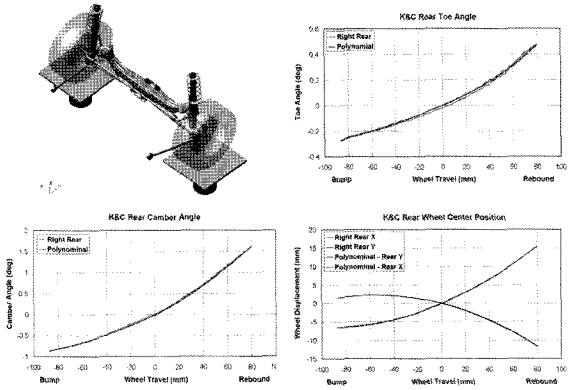

Figure 5. Rear dual-link suspension K&C test results and polynomial fitting.

Figure 4 and Figure 5 show the 3rd order polynomial curve fitting of K&C test results for the front and rear suspensions, respectively.

3.2. Compliance Kinematics

Additional relative displacement of the wheel is the suspension compliant displacement due to longitudinal and lateral force, and aligning moment inputs at tire. The compliance coefficients measured on the K&C test rig are used to construct a compliance matrix.

The amount of the change of wheelbase ($\Delta l'_{w/b}$), tread ($\Delta t'_{w/b}$), camber ($\Delta\alpha'_{w/b}$), and toe angle ($\Delta\gamma'_{w/b}$) are computed.

$$\begin{bmatrix}\Delta l'_{w/b}\\ \Delta t'_{w/b}\\ \Delta\alpha'_{w/b}\\ \Delta\gamma'_{w/b}\end{bmatrix} = \begin{bmatrix}C_{11} & 0 & 0\\ 0 & C_{22} & 0\\ C_{31} & C_{32} & C_{33}\\ C_{41} & C_{42} & C_{44}\end{bmatrix}\begin{bmatrix}F_x\\ F_y\\ M_z\end{bmatrix} \tag{10}$$

where C_{ij} are compliance coefficients.

3.3. Relative Velocity and Acceleration of the Wheel

The functional form of suspension kinematics enables to represent the relative velocity $\dot{y}'_{w/b}$ and acceleration $\ddot{y}'_{w/b}$ in terms of independent velocity $\dot{\delta}_w$, $\dot{s}_r$ and acceleration $\ddot{\delta}_w$, $\ddot{s}_r$. Noting $\dot{y}'_{w/b} = \dot{Z}'_{w/b}$ and $\frac{\partial \dot{Z}'_{w/b}}{\partial \dot{\delta}_w} = \frac{\partial Z'_{w/b}}{\partial \delta_w}$, $\frac{\partial \dot{Z}'_{w/b}}{\partial \dot{s}_r} = \frac{\partial Z'_{w/b}}{\partial s_r}$,

$$\dot{y}'_{w/b} = \frac{\partial \dot{Z}'_{w/b}}{\partial \dot{\delta}_w}\dot{\delta}_w + \frac{\partial \dot{Z}'_{w/b}}{\partial \dot{s}_r}\dot{s}_r = \frac{\partial Z'_{w/b}}{\partial \delta_w}\dot{\delta}_w + \frac{\partial Z'_{w/b}}{\partial s_r}\dot{s}_r \tag{11}$$

Equation (11) can be written in matrix form as

$$\dot{y}'_{w/b} = R_i \dot{q} \tag{12}$$

where $R_i = [R_1 \; R_2] = \left[\frac{\partial Z'_{w/b}}{\partial \delta_w} \; \frac{\partial Z'_{w/b}}{\partial s_r}\right]$, $\dot{q} = [\dot{\delta}_w \; \dot{s}_r]^T$, for the steerable suspension and $R_i = R_1$, $\dot{q} = \dot{\delta}_w$, for the non-steerable suspension.

The relative wheel acceleration can be written as

$$\ddot{y}'_{w/b} = R_i \ddot{q} + h_2 \tag{13}$$

where $h_2 = \frac{\partial^2 Z'_{w/b}}{\partial \delta_w^{\,2}}\dot{\delta}_w^{\,2} + \frac{\partial^2 Z'_{w/b}}{\partial s_r^{\,2}}\dot{s}_r^{\,2} = R_3\dot{\delta}_w^{\,2} + R_4\dot{s}_r^{\,2}$ for the steerable suspension and $h_2 = \frac{\partial^2 Z'_{w/b}}{\partial \delta_w^{\,2}}\dot{\delta}_w^{\,2} = R_3\dot{\delta}_w^{\,2}$ for the non-steerable suspension.

4. VEHICLE DYNAMICS MODEL

4.1. Velocity Transformation

By using equation (5) and equation (6), the wheel velocity and acceleration vector at each corner of the vehicle can be written in terms of generalized velocity and acceleration of the suspension.

$$\dot{y}'_{wi} = D_i \dot{y}'_b + E_i R_i \dot{q}_i \,, \qquad i = 1, \ldots, 4 \tag{14}$$

$$\ddot{y}'_{wi} = D_i \ddot{y}'_b + E_i R_i \ddot{q}_i + h_i \,, \qquad i = 1, \ldots, 4 \tag{15}$$

where $h_i = h_{1i} + E_i h_{2i}$, and i=1 for front right, i=2 for front left, i=3 for rear right, and i=4 for rear left.

The velocity and acceleration of the rack bar of the rack and pinion steering system is written as

$$\dot{y}'_r = D_r \dot{y}'_b + C_r \dot{s}_r \tag{16}$$

$$\ddot{y}'_r = D_r \ddot{y}'_b + C_r \ddot{s}_r + h_r \tag{17}$$

where

$$h_r = \begin{bmatrix} 2\tilde{\omega}'_b \dot{r}'_{r/b} + \tilde{\omega}'_b \tilde{\omega}'_b r'_{r/b} \\ 0 \end{bmatrix}$$

$$C_r = [0 \;\; 1 \;\; 0 \;\; 0 \;\; 0 \;\; 0]^T$$

By collecting all the velocity vectors of the component bodies the Cartesian velocity vector $\dot{y}'_{(36\times1)}$ is written in terms of the generalized velocity vector, $\dot{q}'_{(11\times1)}$ in matrix form

$$\dot{y}' = B\,\dot{q} \tag{18}$$

where B is the velocity transformation matrix

$$B = \begin{bmatrix} I_{6\times6} & 0 & 0 & 0 & 0 & 0 \\ D_1 & E_1R_{11} & 0 & 0 & 0 & E_1R_{21} \\ D_2 & 0 & E_2R_{12} & 0 & 0 & E_2R_{22} \\ D_3 & 0 & 0 & E_3R_{13} & 0 & 0 \\ D_4 & 0 & 0 & 0 & E_4R_{14} & 0 \\ D_r & 0 & 0 & 0 & 0 & C_r \end{bmatrix} \tag{19}$$

The virtual displacement relationship is same as velocity one

$$\delta y' = B \delta q \tag{20}$$

The acceleration vector is written in terms of generalized acceleration vector.

$$\ddot{y}' = B\ddot{q} + H \tag{21}$$

where

$$H = \begin{bmatrix} 0 \\ E_1(R_{31}\dot{\delta}_{w1}^{\,2} + R_{41}\dot{s}_r^{\,2}) + h_{11} \\ E_2(R_{32}\dot{\delta}_{w2}^{\,2} + R_{42}\dot{s}_r^{\,2}) + h_{12} \\ E_3R_{33}\dot{\delta}_{w3}^{\,2} + h_{13} \\ E_4R_{34}\dot{\delta}_{w4}^{\,2} + h_{14} \\ h_r \end{bmatrix}$$

4.2. Equations of Motion

The variational form of equations of motion for the vehicle model in the Cartesian space is written

$$\delta y'^T (M\ddot{y}' - Q) = 0 \tag{22}$$

where

$$M_i = \begin{bmatrix} m_i I & 0 \\ 0 & J'_i \end{bmatrix}, \qquad Q_i = \begin{bmatrix} F'_i \\ n'_i - \tilde{\omega}'_i J'_i \omega'_i \end{bmatrix}$$

M_i is the Cartesian mass matrix and is a constant matrix, and Q_i is the Cartesian generalized force vector. J'_i is the mass moment of inertia, F'_i and n'_i is the Cartesian force and moment vector in each component body's reference frame.

By using equation (20) and (21), equation (22) can be transformed to the generalized coordinate space.

$$\delta q^T (\overline{M}\ddot{q} - \overline{Q}) = 0 \tag{23}$$

where

$$\overline{M} = B^T M B, \qquad \overline{Q} = B^T (Q - MH)$$

Since δq is independent, equation (23) is valid for all

δq. Thus, resulting equations of motion for the vehicle model is

$$\overline{M}\,\ddot{q} = \overline{Q} \tag{24}$$

The detailed multi-body suspension model generates in general differential algebraic equations (DAE). However, equation (24) is an ordinary differential equation (ODE) with 11 degrees of freedom, that is solved by fixed-step integration schemes suitable for real-time simulation.

4.3. Steering Model

In the rack and pinion steering model, the rack bar with pinion is connected to the steering wheel with torsional spring that represents the compliance of torsion bar and steering column. The steering wheel angle input of the driver generates torque applied to the pinion gear that is converted force applied to the rack bar. The rack bar is mounted to the car body with a translational joint with lateral compliance of steering gear mounting bush. A simple power booster curve is used to model power steering.

4.4. Tire Model

The quality of the vehicle dynamics model depends on the tire model. The force and moment generation of the tire-road interface is very complex. The tire model used in this paper is MF-Tire model (Pacejka, 2002).

4.5. Wheel Rotational Dynamics Model

Wheel rotational speed is calculated considering the effects of applied torque (T), rotational inertia (J_w), and tire traction and braking force (F_x) (Chun and Sunwoo, 2004).

$$J_{wi}\dot{\omega}_i = T_i - r_{wi}F_{xi} \tag{25}$$

where r_{wi} is the tire rolling radius. Including wheel rotational degrees of freedom, the vehicle model has 15 degrees of freedom.

4.6. Spring and Damper Model

In this model the spring and damper are connected between car body and wheel center in vertical direction. The nonlinear characteristic of the spring is measured in the K&C ride test. The nonlinear curve with bump and rebound stop is used as spring model. In the damper model, the nonlinear damping curve of the shock absorber is rescaled using the ratio of the wheel travel to the piston stroke of the shock absorber.

5. SIMULATION RESUTLS AND VALIDATION

A passenger car with front McPherson-Strut, rear dual-link suspension, and rack and pinion steering as shown in Figure 1 is modeled using the functional suspension model. The polynomial curve fittings of the K&C test results are shown Figure 5 and Figure 6. In order to verify the validity of the functional suspension model, the simulation results are compared with the analysis results of ADAMS/Car and filed test results for a step steer and Elk test case.

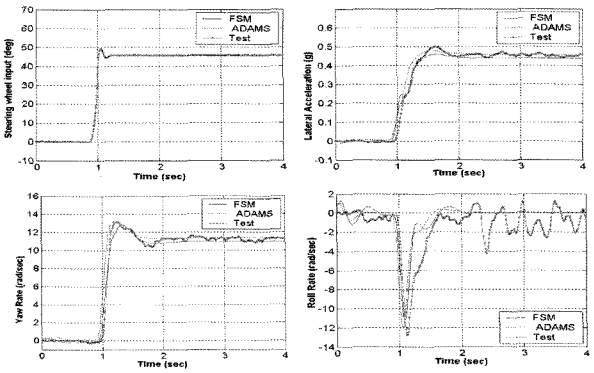

Figure 6. Comparison of step steer responses for ADAMS, FSM and field test.

5.1. Step Steer Simulation

The same step steer (J-turn) input for the test is given to the vehicle model with speed of 82.5 km/h. Figure 6 compares the test results with the simulation results of ADAMS/Car model and FSM (functional suspension model).

The time response of FSM for lateral acceleration, yaw rate, and roll rate shows good correlation with the test results. This demonstrates the validity of the functional suspension model for the handling simulation.

5.2. Step Steer Simulation

The elk test is a severe double lane change maneuver. Using the same steering wheel input of the test, ADAMS/

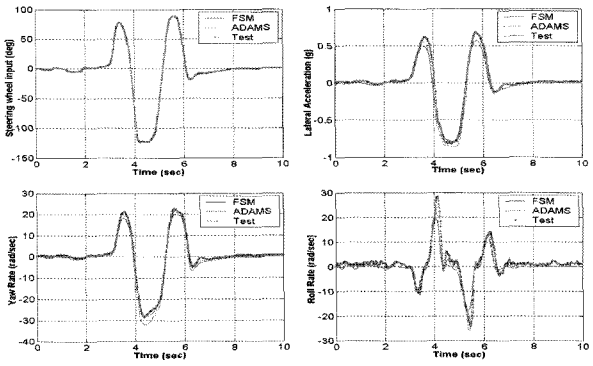

Figure 7. Comparison of elk test responses for ADAMS, FSM and field test.

Car and FSM simulation was performed with a vehicle speed of 68 km/h. Figure 7 shows the comparison of test and simulation results of lateral acceleration, yaw rate, and roll rate. The FSM response gives very good correlation with the test results. Since the peak lateral acceleration reaches 0.75 g, the simulation results of the FSM demonstrates the applicability of the vehicle dynamics model in the highly non-linear handling simulation.

6. APPLICATION TO REAL-TIME ECU EVALUATION SYSTEM

6.1. System Configuration

A ECU evaluation system for semi-active suspension was developed. This HILS system is composed of ECU and solenoid actuator as hardware, Texas Instrument TMS320C6711 150 MHz floating point DSP as a real-time computer, GUI (graphical user interface) computer, and several peripheral boards as shown in Figure 8.

6.2. Semi-active Suspension Control System

A functional diagram of the HILS system for the semi-active suspension control system is shown in Figure 9. The control module, embedded onto the ECU board, receives the sensor signals such as vehicle speed, steering

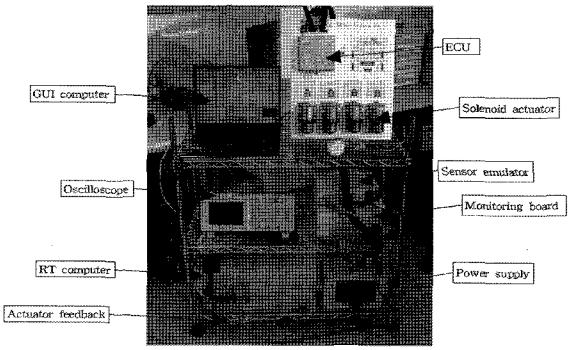

Figure 8. Real-time ECU evaluation system.

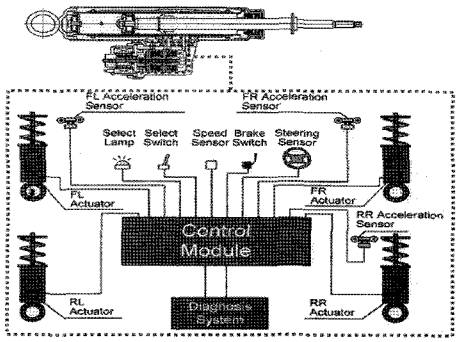

Figure 9. Configuration of HILS system for a semi-active suspension.

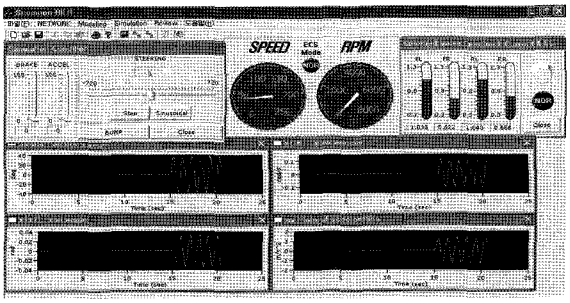

Figure 10. GUI for HILS system control.

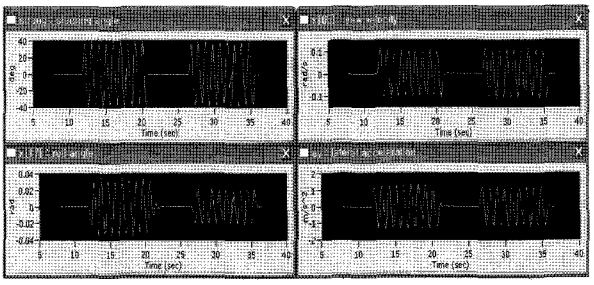

Figure 11. Results of the sinusoidal steering simulation.

wheel angle, throttle position, body vertical accelerations measured at 3 points, mode (sport/normal) select switch position, and brake switch. Then controller generates the lamp signal (on/off) and 4 solenoid current signals calculated through its own logic under the operation environment.

6.3. GUI Computer

GUI computer is used to control real-time ECU evaluation as shown in Figure 10. It starts and stops a simulation, and shows vehicle speed and solenoid currents at each time.

6.4. HILS Simulation Results

In order to evaluate the effectiveness of semi-active suspension control logic in the ECU, hardware-in-the-loop simulation for 1 Hz sinusoidal steering input with 40 deg amplitude at vehicle speed of 40 km/h was performed. In Figure 11, the first part is for the normal

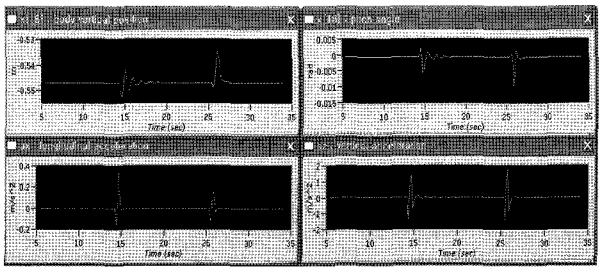

Figure 12. Results of the bump run simulation.

mode and the second part is for the sports mode. The amplitude of roll angle and lateral acceleration are reduced for sports mode.

The bump simulation results are shown in Figure 12. The vehicle runs over the half-sine bump of 0.4m height and 1.2m length at vehicle speed of 40 km/h. The vehicle in sports mode (second part) show higher value of vertical displacement and acceleration and pitch angle of the car body, and stabilizes in shorter time due to higher damping.

7. CONCLUSION

This paper presents an efficient modeling method for real-time vehicle dynamic simulation. A new functional suspension model is proposed as a kinematic describing function of the suspension, that represents the relative wheel displacement in polynomial form in terms of the vertical displacement of the wheel center and steering rack displacement.

The relative velocity and acceleration of the wheel is represented in terms of the first and second derivatives of the kinematic describing function. The equations of motion for the full vehicle model are systematically derived using velocity transformation method. The simulation results of the functional suspension model for step steer and elk test show good correlation with test results. This demonstrates the validity and accuracy of the proposed model.

The vehicle dynamics model based on the functional suspension model is computationally very efficient to achieve real-time simulation on TMS320C6711 150 MHz DSP board on the ECU evaluation system for semi-active suspension.

REFERENCES

Allen, R. W., Rosenthal, T. J. and Szostak, H. T. (1987). Steady state and transient analysis of ground vehicle handling. *SAE Paper No.* 870495.

Choi, B. L., Choi, J. H. and Choi, D. H. (2005). Reliability-based design optimization of an automotive suspension system for enhancing kinematic and compliance characteristics. *Int. J. Automotive Technology* **6**, **3**, 235–242.

Chun, K. and Sunwoo, M. (2004). Wheel slip control with moving sliding surface for traction control system. *Int. J. Automotive Technology* **5**, **2**, 123–133.

Coovert, D. A., Chen, H. F. and Guenther, S. A. (1992). Design and operation of new-type suspension parameter measurement device. *SAE Paper No.* 920048.

Kim, S. S. and Jung, H. K. (2002). Functional suspension modeling and vehicle dynamics analysis using K&C test data. *Spring Conf. Proc., Korean Society of Automotive Engineers*, 855–861, Korea.

Kim, S. S. and Jung, H. K. (2004). Functional suspension modeling for real-time vehicle dynamics analysis using K&C test data. *30th FISITA World Automotive Congress*, Spain.

Kim, S. S. and Vanderploeg, M. J. (1986). A general and efficient method for dynamic analysis of mechanical systems using velocity transformations. *ASME J. Mechanisms, Transmissions, and Automation in Design* **108**, 176–182.

MSC.ADAMS 2003 User's Manual (2003). MSC. Software.

Pacejka, H. B. (2002). Tire and vehicle dynamics. *Society Automotive Engineers*, 172–215.

Sayers, M. W. and Han, D. S. (1996). A generic multibody vehicle model for simulating handling and braking. *Supplement to Vehicle System Dynamics*, **25**, 599–613.